0068

Data-driven motion-corrected brain MRI incorporating pose dependent B0 fields

Yannick Brackenier[1,2], Lucilio Cordero-Grande[1,2,3], Raphael Tomi-Tricot[1,2,4], Tom Wilkinson[1,2], Jan Sedlacik[1,2], Philippa Bridgen[1,2], Sharon Giles[1,2], Shaihan Malik[1,2], Enrico De Vita[1,2], and Joseph V Hajnal[1,2]

[1]Biomedical Engineering Department, School of Biomedical Engineering and Imaging Sciences, King's College London, London, United Kingdom, [2]Centre for the Developing Brain, School of Biomedical Engineering and Imaging Sciences, King's College London, London, United Kingdom, [3]Biomedical Image Technologies, ETSI Telecomunicación, Universidad Politécnica de Madrid and CIBER-BNN, Madrid, Spain, [4]MR Research Collaborations, Siemens Healthcare Limited, Frimley, United Kingdom

Synopsis

A fully data-driven retrospective motion correction reconstruction for volumetric brain MRI at 7T that includes modelling of pose-dependent changes in polarising magnetic (B0) fields in the head has been developed. Building on the DISORDER framework, the use of a physics-based B0 model constrains the number of unknowns to be found, enabling motion correction based solely on data-consistency without requiring any additional probe- or navigator-data. The proposed reconstruction was validated on an in-vivo spoiled gradient echo acquisition in which the subject deliberately moved. Substantial removal of motion artefacts was achieved.

Introduction

Tissue susceptibility causes the polarising magnetic field (B0) in the head to be spatially varying and pose dependent[1], altering the signal acquired in MRI[2]. Although having limited effect for small motion[3] or clinical field strengths[4], these B0 drifts hamper motion correction for increased motion levels at ultra-high field (UHF) and need to be included in the forward model[5]. Navigators and NMR probes have been used to measure pose-dependent fields but require additional hardware and/or scanning time and usually have limited temporal or spatial resolution[6,7]. This work extends the DISORDER motion correction framework[4], which leverages optimized Cartesian sampling, by including a physics-based model to account for pose-dependent B0 fields, resulting in a fully data-driven, retrospective motion correction.

Methods

For volumetric encoding with Cartesian sampling, the DISORDER framework achieves motion correction by dividing k-space profiles (readouts) in temporal segments and allowing each segment to have a distinct motion state. This allows high (sub-second) temporal motion reconstruction as parallel imaging provides an over-determined problem to solve. However, adding a volumetric voxel-based estimation of the spatially varying B0 at every segment would make the reconstruction under-determined and a more compact B0 representation is needed. Building on prior studies[8,9], we observed that relative changes in B0 fields in the moving head frame due to motion at segment s consist of a background field, represented well by lower-degree (2 here) solid harmonics (SH), and localised fields close to air tissue interfaces, which are proportional to the pitch and roll rotation angles θ_{pitch} and θ_{roll} (Fig. 1):

$$\omega_s(\mathbf{r}) = d_{pitch}(\mathbf{r})\theta_{s,pitch} + d_{roll}(\mathbf{r})\theta_{s,roll} + \sum_{n=0}^{2} SH_n(\mathbf{r})c_{n,s} \qquad (1)$$

where $\mathbf{d}(\mathbf{r})$ are the linear maps in $\boldsymbol{\theta}$, SH_n the set of the solid harmonics of degree n with segment-dependent coefficients $c_{n,s}$. $c_{n,s}$ includes pose-dependent B0 effects (e.g. head-body orientation) as well as pose-independent B0 effects (breathing, scanner drift, etc)[10]. Both linear maps $\mathbf{d}(\mathbf{r})$ are smooth and sparse in space, reducing their parameter space even further. B0 fields are estimated based on data-consistency and incorporated in the DISORDER joint image ($\hat{x}$) and rigid motion ($\hat{z}_s$) reconstruction by replacing the Discrete Fourier operator F with a field-dependent Fourier operator F_{ω_s}[11]. For spoiled sequences, the latter reduces to FP_{ω_s} where P_{ω_s} is a segment-dependent phase term. By commuting P_{ω_s} and ST_{z_s}, the phase term is applied in the native image space (head frame), which is consistent with the $\omega_s(\mathbf{r})$ definition:

$$\hat{x}, \hat{z}_s, \hat{\omega}_s = argmin_{x,z_s,\omega_s} \sum_{s'} ||A_{s'} FST_{z_{s'}} P_{\omega_{s'}} x - y_{s'}||_2^2 \qquad (2)$$

where s' sums over all segments and T_{z_s}, S, A_s, y_s respectively represent rigid motion, coil sensitivities, sampled profiles and measured data for segment s, as defined in DISORDER[4]. The DISORDER iterative solver is augmented with a Gradient Descent optimizer for $c_{n,s}$ at every segment and a Fast Iterative Thresholding Algorithm (FISTA)[12] for the regularised $d(\mathbf{r})$ update:

$$d^{i+1} = argmin_d \sum_{s'} ||A_{s'} FST_{z_{s'}} P_{\omega_{s'}} x - y_{s'}||_2^2 + ||d||_1 + ||Dd||_2^2 \qquad (3)$$

where D is the finite-difference operator to enforce smoothness. The proposed reconstruction was tested in simulations and validated in-vivo for a spoiled gradient echo (SPGR) sequence on a 7T scanner (MAGNETOM Terra, Siemens Healthcare, Erlangen, Germany). A volunteer was asked to deliberately move position every 20 seconds. Sequence parameters: 1.5mm isotropic resolution, 0.66s DISORDER motion resolution, TR=10ms, TE=5ms, flip angle FA=7°, FOV=220×240×200 (IS/AP/LR), readout along IS, scan duration TA=2min57s with no repeats and no acceleration.

Results

Fig. 2 shows magnitude images from the different reconstructions. A clear reduction in motion corruption is observed for the proposed motion and B0 corrected reconstructions. This results in an overall increase in contrast and a recovered signal in areas close to air-tissue interfaces.

Only considering the SH does not greatly improve reconstruction (not shown), whereas the linear maps $d(\mathbf{r})$ alone contribute most to the improved image reconstruction. Although motion corruption is reduced when accounting for B0 variation, the proposed reconstruction still contains residual artefacts and lower signal to noise ratio (SNR) compared to a motion-free scan. Linear maps $d_{pitch}(\mathbf{r})$ and $d_{roll}(\mathbf{r})$ are shown in Fig. 3 and agree with the literature[8,13,14] and our own observations from motion-free data both in terms of dynamic ranges (up to 10Hz/degree) and spatial distributions (near air-tissue interfaces). Estimated motion parameters for the different reconstructions are shown in Fig. 4. Including the B0 model in the reconstruction results in more stable and realistic motion traces. Finally, SH coefficient traces are shown in Fig. 5 and follow the motion pattern, with fluctuations superposed, which probably come from confounding factors (e.g. respiration), as previously suggested[5]. This confirms that $c_{n,s}$ includes pose-dependent and pose-independent effects.

Discussion

We have shown improved motion correction for UHF brain imaging by incorporating an explicit pose dependent B0 field term, using a compact physics-based model. Substantial reduction of motion artefacts was achieved in multiple test scans, however, as the conditioning of Equation (3) is determined by the variability of the motion parameters, simulations and in-vivo data show that the added benefit of the proposed reconstruction reduces in scans with little motion.

Conclusion

We have demonstrated the feasibility of fully data-driven retrospective rigid motion correction at UHF by including pose dependent B0 fields. Our method does not require any additional hardware or scanning time and once refined can be easily translated into other sequences.

Acknowledgements

References

1. Liu, J., Zwart, J.D., Gelderen, P.V., Murphy-Boesch, J., & Duyn, J. (2018). Effect of head motion on MRI B0 field distribution. Magnetic Resonance in Medicine, 80, 2538 - 2548.

2. Barmet C., Pruessmann K. (2013). Sensitivity encoding and B0 inhomogeneity - A simultaneous reconstruction approach. Proc. Intl. Soc. Mag. Reson. Med. 13

3. Cordero-Grande L., Tomi-Tricot R., Ferrazzi F., Sedlacik J., Malik S., and Hajnal JV. (2020). Preserved high resolution brain MRI by data-driven DISORDER motion correction. Proc. Intl. Soc. Mag. Reson. Med. 20

4. Cordero-Grande, L., Ferrazzi, G., Teixeira, R.P., O'Muircheartaigh, J., Price, A., & Hajnal, J. (2020). Motion-corrected MRI with DISORDER: Distributed and incoherent sample orders for reconstruction deblurring using encoding redundancy. Magnetic Resonance in Medicine, 84, 713 - 726.

5. Liu, J., Gelderen, P., Zwart, J.D., & Duyn, J. (2019). Reducing motion sensitivity in 3D high-resolution T2*-weighted MRI by navigator-based motion and nonlinear magnetic field correction. NeuroImage, 116332 .

6. Wallace, T.E., Afacan, O., Kober, T., & Warfield, S. (2019). Rapid measurement and correction of spatiotemporal B0 field changes using FID navigators and a multi-channel reference image. Magnetic Resonance in Medicine, 83, 575 - 589.

7. Sipilä, Pekka Tapani et al. "Robust, susceptibility-matched NMR probes for compensation of magnetic field imperfections in magnetic resonance imaging (MRI)." Sensors and Actuators A-physical 145 (2008): 139-146.

8. Sulikowska, A. (2016). Motion correction in high-field MRI. PhD thesis, University if Nottingham.

9. Marques, J., & Bowtell, R. (2005). Application of a Fourier-based method for rapid calculation of field inhomogeneity due to spatial variation of magnetic susceptibility. Concepts in Magnetic Resonance Part B-magnetic Resonance Engineering, 25, 65-78.

10. Moortele, P.V., Pfeuffer, J., Glover, G., Ugurbil, K., & Hu, X. (2002). Respiration-induced B0 fluctuations and their spatial distribution in the human brain at 7 Tesla. Magnetic Resonance in Medicine, 47.

11. Matakos, A., & Fessler, J. (2010). Joint estimation of image and fieldmap in parallel MRI using single-shot acquisitions. 2010 IEEE International Symposium on Biomedical Imaging: From Nano to Macro, 984-987.

12. Beck, A., & Teboulle, M. (2009). A Fast Iterative Shrinkage-Thresholding Algorithm for Linear Inverse Problems. SIAM J. Imaging Sci., 2, 183-202.

13. Andersson, J., Graham, M., Drobnjak, I., Zhang, H., & Campbell, J. (2018). Susceptibility-induced distortion that varies due to motion: Correction in diffusion MR without acquiring additional data. Neuroimage, 171, 277 - 295.

14. Yarach, U., Luengviriya, C., Stucht, D., Godenschweger, F., Schulze, P., & Speck, O. (2015). Correction of B0-induced geometric distortion variations in prospective motion correction for 7T MRI. Magnetic Resonance Materials in Physics, Biology and Medicine, 29, 319-332.
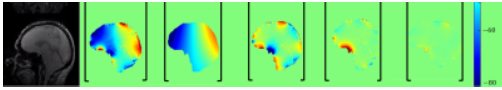
Figures
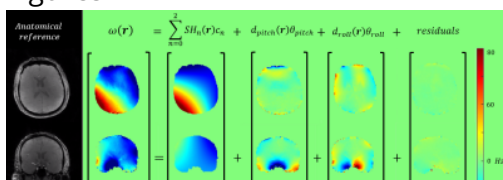
Figure 1: Relative B0 field changes $\omega(\mathbf{r})$ in the head frame between two poses, obtained after registration, can be decomposed in lower-degree solid harmonics (n=2) and localised fields that are proportional to rotation angles θ_{pitch} and θ_{roll} (12 and 10 degrees for this example). The linear model $d(\mathbf{r})$ (not shown here) was fitted on a total of 8 motion-free scans. Data shown here is not used in further reconstructions and only served to validate our model.
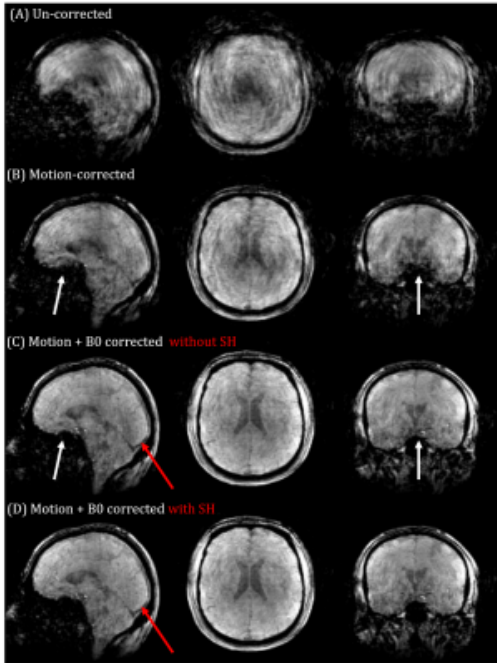
Figure 2: Sagittal (left), transversal (middle) and coronal (right) view of the (A) uncorrected (B) motion-corrected and proposed motion + B0 reconstruction (C) without and (D) with considering the solid harmonics (SH). Reduced motion corruption is observed when including the pose-dependent B0 fields with the biggest contribution coming from the linear B0 model, resulting in recovered signal near air-tissue interfaces (white arrows) and improved contrast, e.g. around the ventricles. Residual improvements are obtained when including the solid harmonics (red arrows).
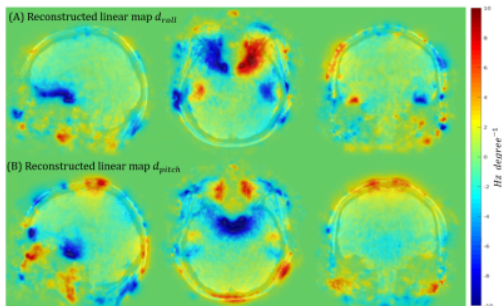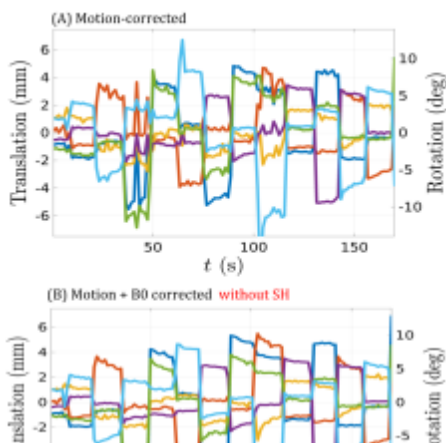

Figure 3: Reconstructed linear maps $\mathbf{d}(\mathbf{r})$ for (A) pitch and (B) roll rotation angles θ_{pitch} and θ_{pitch} overlaid on the reconstructed anatomical image. Strong linearity is observed close to air-tissue boundaries, whereas the induced fields deeper in the brain are characterized better by the lower-degree solid harmonics.
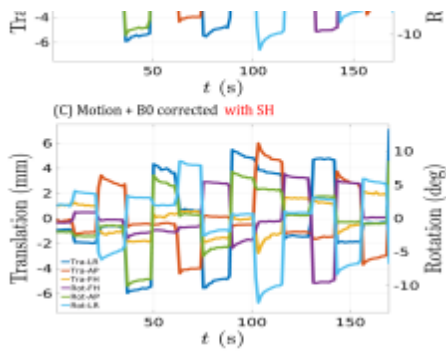
Figure 4:Translation and rotation motion traces for the (A) motion-corrected and proposed motion + B0 reconstruction (B) without and (C) with considering the solid harmonics (SH). Foot Head (FH), Anterior-Posterior (AP) and Left-Right (LR) rotations respectively represent yaw, roll and pitch rotation. More accurate motion parameters are obtained from the proposed reconstruction as the oscillatory motion traces are in discrepancy with instructions given to the volunteer. Substantial improvements come from the linear B0 model compared to the improvements of the SH.
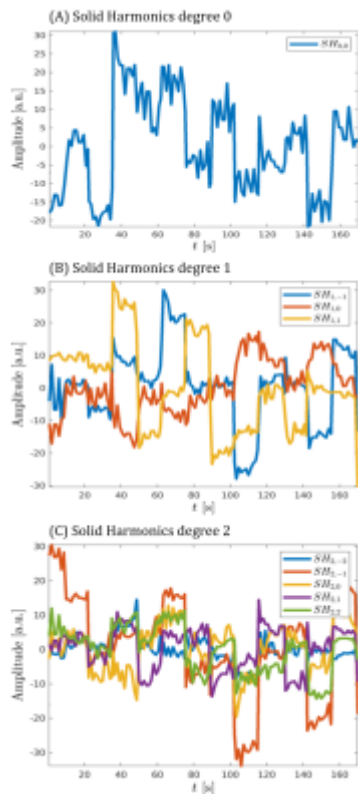

Figure 5: Temporal coefficients of the solid harmonics $SH_{n,m}$ of degree n and order m B0 fields. Solid harmonics are defined so that the $SH_{1,-1}$, $SH_{1,0}$ and $SH_{1,1}$ respectively represent a linear field in the AP, HF and LR direction. Coefficients follow the motion pattern, with superposed fluctuations probably coming from the confounding factors such as respiration, as has been reported previously[5].